Signaling pathways controlling activity-dependent local translation of BDNF and their localization in dendritic arbors

Gabriele Baj, Vera Pinhero, Valentina Vaghi and Enrico Tongiorgi*

ABSTRACT

Brain-derived neurotrophic factor (BDNF) is encoded by multiple mRNA variants whose differential subcellular distribution constitutes a 'spatial code' for local translation of BDNF and selective morphological remodeling of dendrites. Here, we investigated where BDNF translation takes place and what are the signaling pathways involved. Cultured hippocampal neurons treated with KCl showed increased BDNF in the soma, proximal and distal dendrites, even in quaternary branches. This activity-dependent increase of BDNF was abolished by cycloheximide, suggesting local translation, and required activation of glutamate and Trk receptors. Our data showed that BDNF translation was regulated by multiple signaling cascades including RAS–Erk and mTOR pathways, and CaMKII–CPEB1, Aurora-A–CPEB1 and Src–ZBP1 pathways. Aurora-A, CPEB1, ZBP1 (also known as IGF2BP1), eiF4E, S6 (also known as rpS6) were present throughout the dendritic arbor. Neuronal activity increased the levels of Aurora-A, CPEB1 and ZBP1 in distal dendrites whereas those of eiF4E and S6 were unaffected. BDNF-6, the main dendritic BDNF transcript, was translated in the same subcellular domains and in response to the same pathways as total BDNF. In conclusion, we identified the signaling cascades controlling BDNF translation and we describe how the translational machinery localization is modulated in response to electrical activity.

KEY WORDS: Neurotrophins, Hippocampus, Protein synthesis, Pilocarpine

INTRODUCTION

Translation of a subset of dendritically localized mRNAs in close proximity to activated synapses is a fundamental mechanism to enable selective synaptic changes underlying learning and memory. Among the mRNAs that are translated in dendrites, brain-derived neurotrophic factor (BDNF) is of particular interest for its implication in development, cell survival and plasticity of the nervous system. Growing evidence indicates that local protein synthesis of BDNF is a key event for an extensive reorganization of dendrite arborization and spine morphology (An et al., 2008; Baj et al., 2011; Kellner et al., 2014; Sun et al., 2014; Verpelli et al., 2010; Xu et al., 2014). Translation of neuronal mRNAs localized in dendrites is controlled by signaling cascades activated by glutamate receptors and BDNF itself (Bramham and Wells, 2007; Leal et al., 2014). Translation of BDNF mRNA requires interaction with the

Department of Life Sciences, B.R.A.I.N. Centre for Neuroscience, University of Trieste, Trieste 34127, Italy.

*Author for correspondence (tongi@units.it)

G.B., 0000-0002-2625-9454; V.P., 0000-0003-1754-6360; E.T., 0000-0003-0485-0603

binding protein HuD (also known as ELAVL4), which is mediated by a protein kinase C (PKC)-dependent pathway (Lim and Alkon, 2012), and phosphorylation of the eukaryotic elongation factor (eEF2) by the eEF2 kinase (eEF2K), two key pathways involved in synaptic plasticity (Verpelli et al., 2010). However, it is still unclear how the different signaling cascades controlling translation can regulate BDNF and where these signaling pathways are active in the different subcellular regions. The question of how and where protein synthesis occurs in neurons is of general interest because neurons have a distinctive, highly polarized cellular morphology, with complex dendritic arborization characterized by primary, secondary and higher order ramifications (Baj et al., 2014; Cáceres et al., 2012; Fiala et al., 2007). Given that different types of synapses (glutamatergic GABAergic, cholinergic, etc.) are differentially distributed along the dendritic arbor (Megías et al., 2001), the localization of the translational machinery is crucial because it can specifically affect distinct neuronal networks. For instance, the distal dendritic compartment contains >90% of the excitatory synapses of a pyramidal neuron (Megías et al., 2001). However, it has been suggested that BDNF translation might occur only in the proximal segment of dendrites because some elements of the translational machinery are supposedly excluded from the most distal, high-order (tertiary and quaternary) dendritic branches (Lu et al., 1991). In contrast to this view, protein translation and glycosylation were demonstrated to occur even in distal dendritic compartments (tom Dieck et al., 2015; Torre and Steward, 1992; Torre and Steward, 1996).

Transcription of the *Bdnf* gene generates multiple mRNA splice variants (Aid et al., 2007). We have previously proposed that the BDNF mRNA variants provide a 'spatial code' for a segregated expression within three neuronal compartments: the soma (BDNF variants 1, 3, 5, 7, 8 and 9a), the proximal (BDNF variant 4) or the distal dendrites (BDNF variant 2 and 6) (Baj et al., 2013, 2011). Accordingly, we have shown that BDNF-6 trafficking to dendrites is increased by physical exercise and chronic antidepressant treatments (Baj et al., 2012). Moreover, we have demonstrated that BDNF variant 2 and BDNF variant 6 are translated in dendrites and are able to control the morphology of distal dendrites (Baj et al., 2011). In this study, we investigated the sites of activity-dependent translation of endogenous BDNF in dendrites, and identified the key pathways driving activity-dependent translation of BDNF and their subcellular localization under resting conditions and following neuronal activity.

RESULTS

Sites of BDNF translation upon neuronal activity

To determine the specificity of the monoclonal antibody (B5050, Sigma-Aldrich) used to investigate the sites of endogenous BDNF protein synthesis, immunofluorescence was carried out in primary cultures of hippocampal neurons from mice with a floxed BDNF-coding sequence (BDNF$^{lox/lox}$; Gorski et al., 2003). Anti-BDNF

labeling was absent when BDNF[lox/lox] neurons were co-transfected with GFP and Cre-lox recombinase to selectively knockout BDNF (Fig. 1A, green neuron, white arrow; n=2 cultures, about 50 neurons per culture), whereas untransfected neurons within the same culture showed labeling for BDNF on soma and dendrites (Fig. 1A, black arrows). Anti-BDNF antibody showed a residual fluorescence intensity of ~27±8% (mean±s.e.m., n=2 cultures, ~50 neurons per culture) with respect to the untransfected neurons (set as 100%). The reactivity of this monoclonal antibody was further tested by western blot analysis on homogenates from primary cultures of rat

hippocampal neurons at 14 days *in vitro* (DIV14). Anti-BDNF antibody was able to recognize all BDNF isoforms, namely proBDNF (32 kDa), truncated BDNF (also known as pro28, 28 kDa) and mature BDNF (14 kDa) (Fig. 1B). To induce an activity-dependent increase in endogenous BDNF, DIV14 rat neurons were stimulated either for 15 min or 3 h with high K^+ (K^+ solution, 50 mM KCl) and the total BDNF protein levels from n=3 independent cultures was quantified by an ELISA assay which recognizes both pro- and mature BDNF protein forms (Polacchini et al., 2015, Fig. 1C). After 15 min KCl stimulation, total BDNF
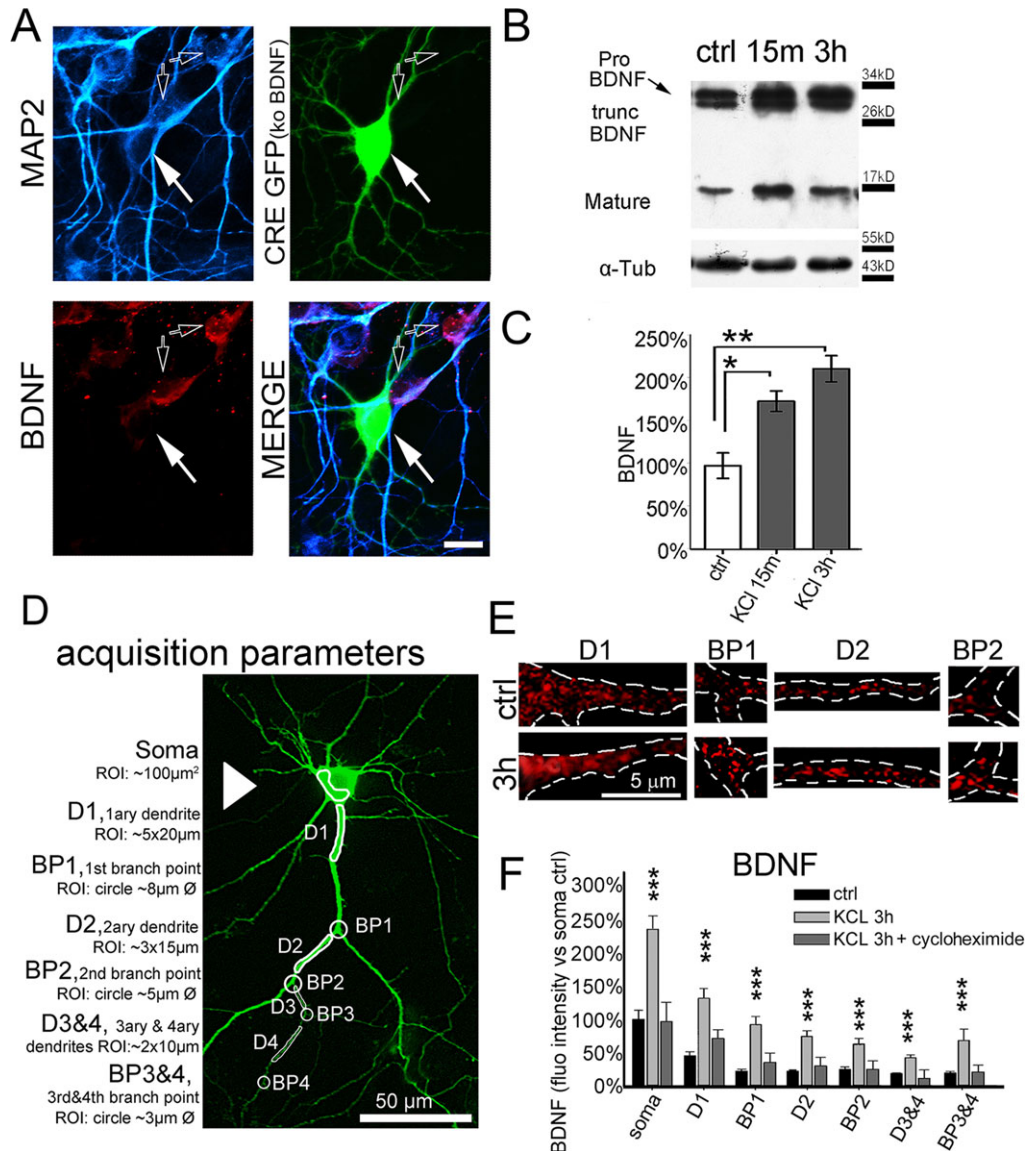
Fig. 1. Anti-BDNF antibody specificity, BDNF translation and localization. (A) Hippocampal neurons from BDNF[lox/lox] mice stained for MAP2 (cyan), GFP (green, positive control for transfection for recombinase) and BDNF (red). Neurons transfected with Cre-recombinase are BDNF-depleted (white arrow) whereas untransfected neurons can produce BDNF (black arrows). Scale bars: 10 μm. (B) Left panel, western blot analysis, using anti-BDNF and anti-α-tubulin antibodies (both from Sigma), of protein extracts from rat hippocampal neurons maintained for 14 days *in vitro* (14 DIV) and stimulated on the last day with 50 mM K^+ solution for 15 min and for 3 h, respectively. Control (ctrl) refers to untreated neurons. The black arrow points out BDNF isoforms. Positions of the molecular mass markers (kD) are indicated. (C) ELISA assay quantification of BDNF in DIV14 rat hippocampal neurons following depolarization by KCl (50 mM K^+ solution) for 15 min and for 3 h (n=3). (D) Representative GFP-transfected neuron showing the subcellular regions of interest (ROIs) designed for the densitometric analysis. (E) Representative image of immunofluorescence labeling for BDNF in the ROIs for the subcellular domains D1, BP1, D2, and BP2, in control and stimulated conditions. (F) Densitometric analysis of BDNF immunofluorescence in control conditions, when stimulated with K^+ solution 50 mM for 3 h and in presence of cycloheximide (50 μg/ml). The recorded staining in the different ROIs has been normalized for Map2 and on the ratio of BDNF to Map2 measured in the soma of control neurons (set as 100%). Data are expressed as mean±s.e.m. (n=24 neurons from three cultures for each condition). ***P<0.001 (one-way ANOVA followed by a multiple comparison versus control group procedure with Holm-Sidak's method).

was 176.25±8.36% and was 215.84±12.65% at 3 h, with respect to control conditions taken as 100±12.36% (Fig. 1C). Given that there was no statistically significant difference between 15 min and 3 h in total BDNF levels all subsequent experiments were carried out at 3 h.

The local production of BDNF in the different somato-dendritic compartments of rat hippocampal neurons was analyzed using immunofluorescence and high-resolution confocal imaging followed by densitometric quantification within regions of interest (ROIs) whose design parameters are described in detail in Fig. 1D. The seven subcellular domains defined by these ROIs are soma, primary dendrites (D1), first branch points (BP1), secondary dendrites (D2), second branch points (BP2), tertiary and quaternary dendrites (D3&4), and third and fourth branch points (BP3&4). The densitometry data were normalized to the BDNF immunofluorescence level recorded in the soma of control cells. Therefore, we were able to measure both the relative protein distribution from soma to dendritic regions and the variations from control to stimulated conditions. A significant increase in BDNF immunofluorescence was observed after 3 h KCl treatment in all regions of interest (Fig. 1E,F; $P<0.001$, $n=24$ neurons from 3 cultures for each condition). BDNF immunofluorescence progressively declined with increasing distance from the soma becoming less pronounced in tertiary and quaternary dendrites although it remained elevated in the third and fourth branch points. In particular, the greatest increase following KCl was seen in the first branch points (+308.1±51.7%) when taking control conditions for BP1 as 100% and in the tertiary and quaternary branch points (+242.5±84.6%), when taking control conditions for BP3&4 as 100%. These findings indicate that in proximal dendrites BDNF translation can equally occur in the dendritic shaft and branch points whereas in the periphery of the dendritic arbor, BDNF translation is preferentially localized at branching points. To verify whether these phenomena were a specific effect of increased BDNF translation, we pre-treated neurons 30 min prior to KCl administration with the protein translation inhibitor cycloheximide. In these conditions, the KCl-induced increase in BDNF was abolished and no significant differences in BDNF levels and distribution with respect to untreated neurons was observable in any cellular district (Fig. 1F).

Signaling pathways activating endogenous BDNF mRNA translation

Local translation in the dendritic compartment can be controlled by multiple signaling cascades activated by glutamate receptors and BDNF itself (Bramham and Wells, 2007). These signaling cascades are known to regulate translation by modulating effector proteins interacting with the 5′ or the 3′ untranslated regions (UTR) of dendritic mRNAs (Bramham and Wells, 2007). Fig. 2A shows some of these pathways and the specific inhibitors that we used to study how translation of endogenous BDNF is controlled in dendrites of DIV14 rat hippocampal neurons. In the first set of experiments, we tested the hypothesis that BDNF translation could be triggered by activation of glutamate receptors. Incubation of DIV14 rat hippocampal neurons with KCl for 3 h induced an increase in total BDNF of +221±13% with respect to the endogenous basal levels (100%) measured by ELISA from hippocampal culture homogenates (Fig. 2B; mean±s.e.m, $n=3$ experiments from three cultures). Inhibitors of glutamate receptors of the NMDA type (Kin Ac, 1 mM) or AMPA type (DNQX, 20 µM) were added to the medium 30 min prior to KCl-induced depolarization and both drugs alone, or in combination, fully blocked the KCl-induced BDNF increase (Fig. 2B). The KCl-induced increase in BDNF translation was also blocked by K252a, an inhibitor of Trk receptors, indicating a role of neurotrophins in the regulation of BDNF synthesis (Fig. 2B).

Having established that BDNF translation is induced by the typical signaling cascades of excitatory synapses, (i.e. those triggered by glutamate receptors and neurotrophins) we focused on the downstream signaling cascades. Inhibition of signaling mediated by the Ras, Erk 1 and Erk2 (Erk1/2, also known as MAPK3 and MPAK1, respectively) and eukaryotic initiation factor 4E (eiF4E) (U0126 inhibitor), the phosphoinositide 3-kinase (PI3K), mammalian target of rapmycin (mTOR) and S6K (Rapamycin), or the phospholipase C (PLC), calmodulin (CaM) and eEF2 (GF inhibitor) pathways, which all control translation through 5′UTR-dependent mechanisms, caused a similar inhibition of BDNF translation. Comparable results were also achieved by inhibiting signaling cascades involving regulation at the 3′UTR, namely that regulated by calmodulin-dependent protein kinase II (CaMKII) and CPEB1 (KN62 inhibitor), Aurora-A and CPEB1 (AuA inhibitor PHA-680632), or Src and ZBP1 (also known as IGF2BP1) (PP2 inhibitor). These assays were also performed using UO124 (the inactive form of UO126), SU5402 (an FGFR inhibitor) or SB505124 (an TGFβR inhibitor). These compounds did not show any significant effect on BDNF translational regulation in our experimental set-up, indicating that only the inhibition of specific intracellular cascades is able to block BDNF translation (Fig. 2C). Of note, treatments with the inhibitors in absence of KCl did not modify the basal level of BDNF in hippocampal neurons lysates. These results indicate that BDNF is translated in response to multiple, but specific, signaling cascades.

Localization of signaling cascades activating BDNF translation *in vitro*

To determine whether the signaling cascades involved in BDNF translation are locally available in dendrites at resting conditions and after KCl-induced depolarization, we analyzed the distribution of the downstream effectors for each cascade in the different dendritic compartments of DIV14 rat hippocampal neurons (Fig. 3; for each condition, $n=30$ neurons from three cultures). These downstream effectors are RNA-binding proteins that are expected to interact with either the 5′UTR (eiF4E or S6, also known as rpS6) or the 3′UTR (CPEB1, ZBP1 or Aurora-A) of BDNF mRNA (Fig. 3A). We used antibodies previously validated for immunofluorescence (see references in Materials and Methods). However, the anti-Aurora-A antibody was only validated for western blotting (Polacchini et al., 2016) and, therefore, we provided further evidence that confirmed its specificity in immunocytochemistry (Fig. S1D). Control experiments in which the primary antibodies were omitted showed no relevant staining of anti-rabbit-IgG, anti-mouse-IgG or anti-goat-IgG secondary antibodies (Fig. S1A,B,C). Data were acquired and normalized to MAP2 staining in the somata of control neurons as described for BDNF staining. The global translational regulator eiF4E was mostly concentrated in the soma and in the perisomatic area but could be also detected, although to a lesser extent, in dendritic distal regions (Fig. 3B). The staining levels for eiF4E remained constant even after KCl stimulation. Conversely, the ribosomal protein S6 was uniformly distributed throughout all dendritic domains in control conditions and there was no change in soma and dendrites after 3 h stimulation, besides a slight decrease in the proximal primary dendrites (D1; Fig. 3C). Thus, the global regulators of translation, eiF4E and the ribosomes identified by the S6 protein, are distributed in the entire dendritic arborisation and their localization is not modulated by activity.
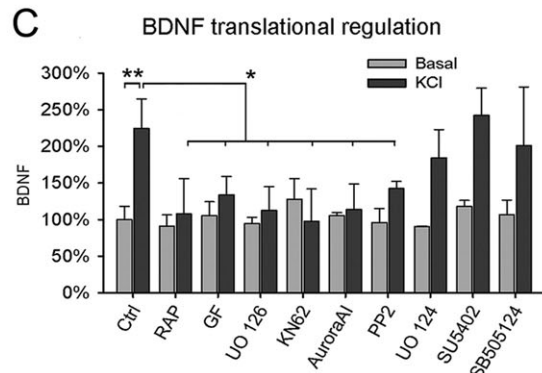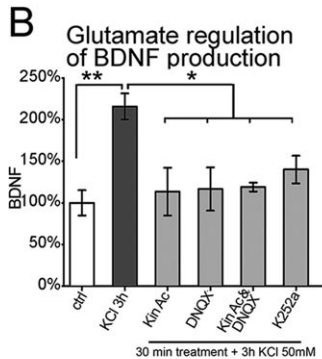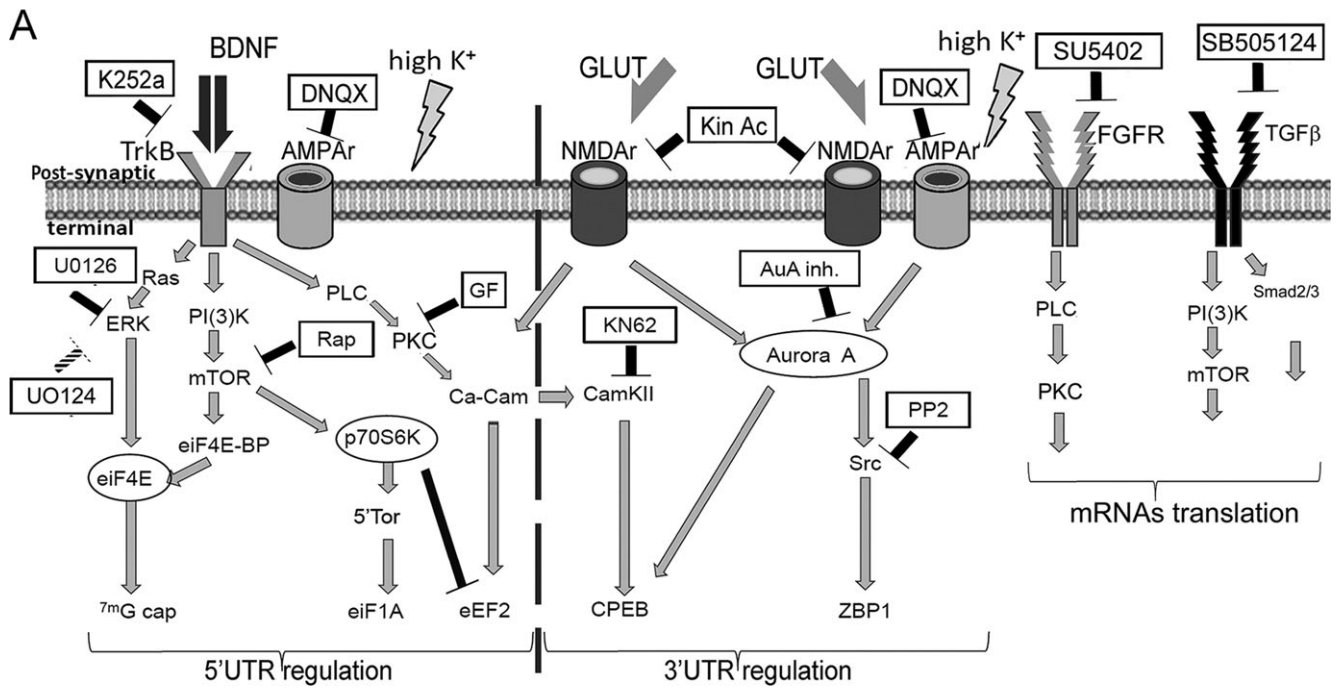
Fig. 2. Pharmacological analysis of the different signaling pathways that activate endogenous BDNF translation. (A) Model of control of dendritic protein synthesis at excitatory synapses in the mammalian brain. Modified from Bramham and Wells (2007). The illustration also reports the inhibitors (boxed) used in the subsequent experiments shown in B and C and the effector proteins analyzed in Fig. 3 (circled). (B) Glutamatergic regulation of BDNF translation. ELISA assay quantification of BDNF in DIV14 rat hippocampal neurons following depolarization by KCl in the presence of the glutamate receptor inhibitors kinurenic acid (KinAc) and DNQX or the Trk receptor inhibitor K252a. (C) BDNF translational regulation. ELISA assay quantification of BDNF in DIV14 rat hippocampal neurons following depolarization (50 mM KCl for 3 h) in the presence of control drug (UO124) or intracellular (UO126, Rap GF,KN62, AuroraA inhib, PP2) and extracellular (SU5402, SB505124) inhibitors of pathways controlling translation. All inhibitors were added to neuronal cultures 30 min before KCl depolarization. Data are expressed as mean±s.e.m. (n=3 experiments from three cultures). *$P<0.05$, **$P<0.01$ (one-way ANOVA followed by a multiple comparison versus control group procedure with Holm-Sidak's method).

We next investigated the distribution of Aurora A, a kinase able to relieve translational repression of mRNAs containing cytoplasmic polyadenylation element (CPE) sequences that are bound by CPEB proteins. In resting neurons, Aurora A was mostly concentrated in the soma with low levels in dendrites (Fig. 3D). Upon 3 h KCl stimulation, Aurora A expression showed a slight but significant increase of 8–18±4% in all dendritic ROIs with respect to the corresponding compartments in control conditions ($P<0.001$, except for the first branch point BP1 in which $P<0.05$; Fig. 3D). Finally, we investigated the subcellular distribution of ZBP1 and CPEB1, two RNA-binding proteins (RBPs) which can control translation of neuronal mRNAs in dendrites by interacting with their 3′UTR. Both RBPs already showed high levels of staining in distal dendritic compartments at rest and KCl treatment induced no variation in the soma but a particularly strong increase in distal dendritic compartments (secondary, tertiary and quaternary dendrites and branch points; Fig. 3E,F). Thus, 3′UTR-dependent translational regulators are modulated upon electrical activity by increasing their localization in the most distal dendritic compartments.

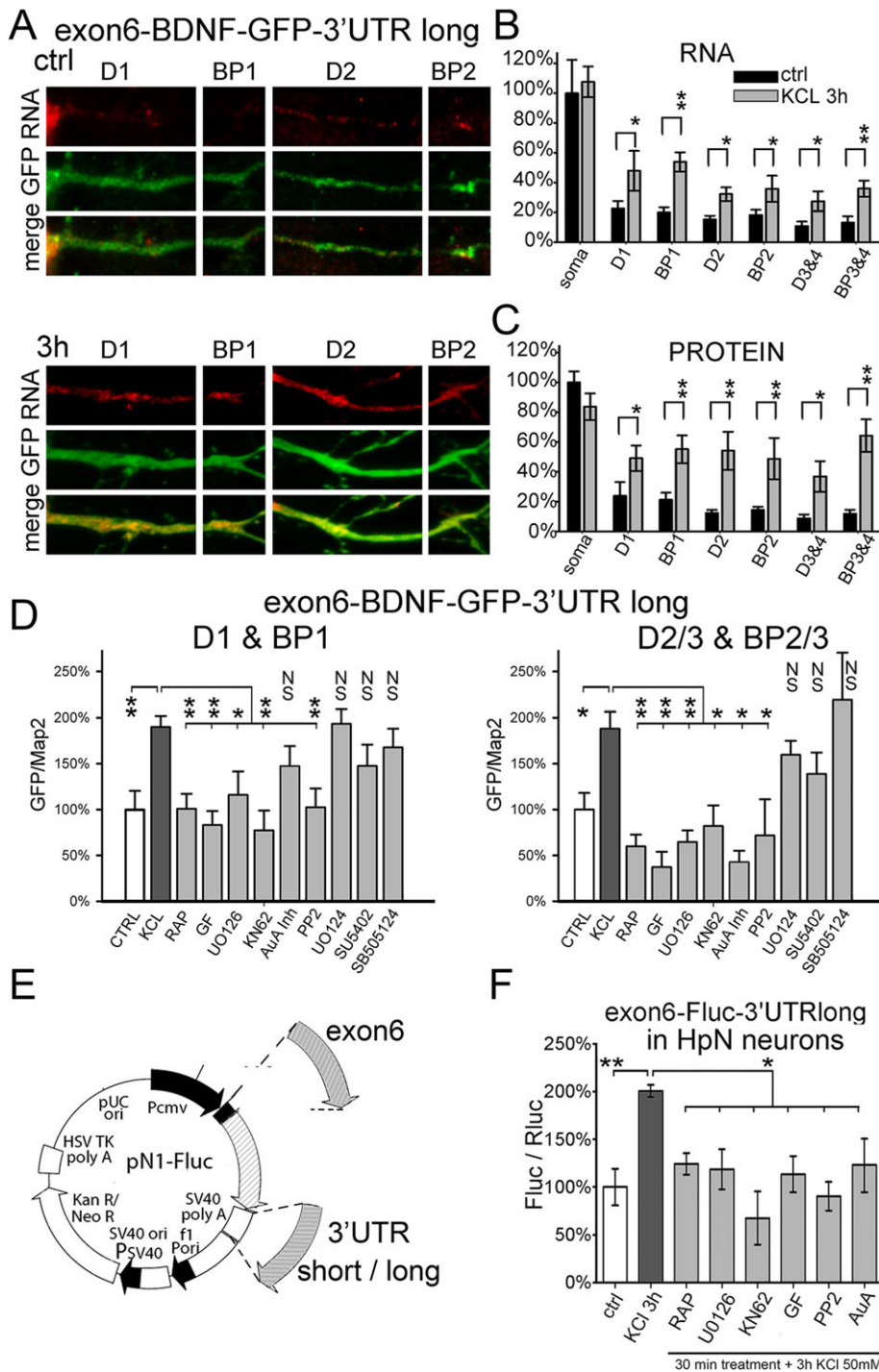### Translational regulation of BDNF exon 6 transcript
The experiment described in the previous paragraphs identified the subcellular compartments in which the different signaling cascades regulating BDNF translation are activated by excitatory activity. To further confirm that the different signaling cascades can control BDNF translation in distal dendrites, we considered the BDNF transcript encoding exon 6 which is the main variant located in dendrites following activity (Baj et al., 2013, 2011). For these experiments, we transfected rat hippocampal neurons with the
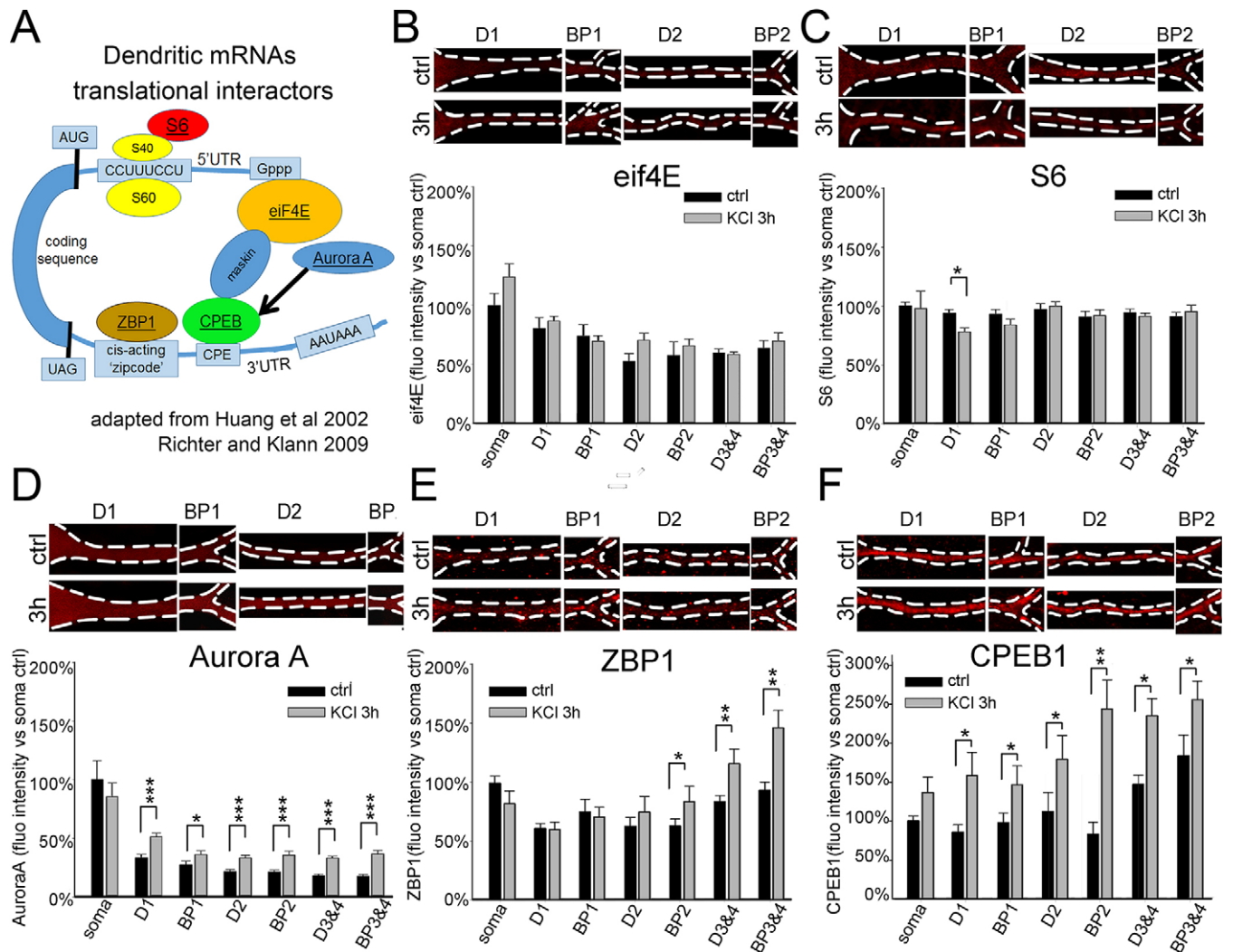
Fig. 3. Translation machinery localization following KCl depolarization. (A) Graphical representation of the investigated molecular interactors involved in mRNA translational control, adapted from Huang et al., 2002 and Richter and Klann, 2009. (B–F) Upper panels, representative magnifications of immunofluorescence staining for the indicated proteins in the subcellular domains D1, BP1, D2, and BP2, under control (ctrl) and stimulated conditions for eiF4E (B), S6 (C), Aurora kinase A (D), ZBP1 (E) and CPEB1 (F). Bottom panels, corresponding densitometric quantification of the immunofluorescence staining for the indicated proteins. Densitometric analysis of immunofluorescence in the different ROIs has been normalized to the intensity measured in soma of control neurons. Data are expressed as mean±s.e.m. gray values (n=30 neurons from three cultures). *P<0.05, **P<0.01, ***P<0.001 (one-way ANOVA).

chimeric constructs denoted exon-6-CDS–GFP–3′UTRlong, containing the 5′UTR (exon 6) and 3′ UTR long regulatory sequences as well as a GFP sequence. Using a similar construct, missing the 3′UTR long sequence, we have previously shown that local protein synthesis of BDNF can occur in dendrites even when they are mechanically severed from the soma (Baj et al., 2011). The localization of the exogenous exon-6-BDNF–GFP mRNA and protein was visualized by dual fluorescence for *in situ* hybridization and immunohistochemistry, with an anti-GFP riboprobe or anti-GFP antibody, respectively (Fig. 4A). Following 3 h KCl stimulation, densitometric analysis revealed an increase in dendritic localization of both exon 6 chimeric mRNA and protein in all compartments whereas no change in protein or mRNA levels could be observed in the soma (Fig. 4B,C; n=30 neurons from three cultures for each condition). Given that no change was detected in the soma, we concluded that the protein increase for this chimeric construct could be accounted for by translation in dendrites. In a subsequent set of experiments, we investigated the contribution of each signaling cascades to the regulation of exon 6 transcript

translation in DIV14 rat hippocampal neurons. To this aim, the experiments shown in Fig. 4C were repeated using the same panel of drugs previously used to inhibit endogenous BDNF translation (see Fig. 2C, for comparison). In these experiments (n=2 cultures, 10 neurons) we focused on BDNF regulation in proximal dendrites (D1 and BP1, Fig. 4D, left panel) and distal dendrites (D2, D3, BP2 and BP3, Fig. 4D, right panel). Similar to the endogenous BDNF, BDNF–GFP translation from BDNF 6 was also blocked by all drugs in distal dendrites and by all drugs but not the Aurora kinase inhibitor PHA-680632 in proximal dendrites. Importantly, no effects on BDNF levels could be seen with the non-active control drug UO124 or with inhibitors of the FGF and TGF-β pathways. To confirm these results, we exploited a luciferase assay that we previously described (Vaghi et al., 2014) in which translation of BDNF is dictated by its 5′UTR and 3′UTR sequences and the BDNF coding region has been replaced by the firefly luciferase coding region (exon-6-Fluc–3′UTRlong; Fig. 4E). Pharmacological inhibition of the individual signaling cascades considered (shown in Fig. 2A), caused a complete suppression of

Fig. 4. Exon6 BDNF transcripts translational regulation. (A) Representative fluorescent *in situ* hybridization (FISH) and immunostaining for GFP (RNA and protein) in DIV14 rat hippocampal neurons transfected with the exon6-BDNF–GFP–3′UTR construct, in control (ctrl) and KCl (50 mM for 3 h) conditions. (B,C) Densitometric analysis of GFP mRNA (B) and GFP protein (C) in the different ROIs normalized to the intensity measured in the soma of control neurons. Data are expressed as mean±s.e.m (*n*=30 neurons from three cultures for each condition). (D) Densitometric analysis of GFP protein in the D1+BP1 area and in the D2, D3, BP2 and BP3 area in the presence of control drug (UO124) or intracellular (UO126, Rap GF,KN62, AuroraA inhib, PP2) and extracellular (SU5402, SB505124) inhibitors of pathways controlling translation. The staining in the ROIs has been normalized for Map2 and to the ratio of BDNF to Map2 measured in the soma area of control neurons. Data are expressed as mean±s.e.m (*n*=10 neurons from two cultures). (E) Firefly luciferase reporter vector design for translational analysis of BDNF exon6 5′UTR and 3′UTR short or long (adapted from Vaghi et al., 2014). (F) Quantification of luciferase assay results in DIV14 rat hippocampal neurons transfected with Exon6-FLuc-3′UTRlong vector in control, stimulated with KCl 50 mM for 3 h, and stimulated in the presence of inhibitors of the different pathways controlling translation. Luciferase assays were performed in primary cells co-transfected with *Renilla* luciferase for normalization. Data are expressed as mean± s.e.m (*n*=2 experiments from two cultures). *P<0.05; **P<0.01; NS, not significant (one-way ANOVA).

translation induced by KCl stimulation (Fig. 4F, *n*=3). These results indicate that translation of BDNF exon 6 requires activation of multiple signaling cascades.

Localization of BDNF translation signaling cascades *in vivo*

The localization of the translational signaling cascades involved in BDNF protein synthesis was also investigated in the rat hippocampus *in vivo* (Fig. 5). To this aim, we quantified the expression and localization of the same elements already studied *in vitro*, in resting animals (saline injected) or after a 3 h-long status epilepticus produced by pilocarpine, an *in vivo* model of massive neuronal activation (Fig. 5; *n*=3 saline-injected and *n*=3

pilocarpine-treated rats, *n*=3–5 brain sections for each animal). The *in vivo* densitometric analysis was carried out on the different hippocampal layers of the CA1 namely, the stratum piramidalis containing the somata; the proximal radiatum, the distal radiatum and the stratum lacunosum-moleculare. In basal conditions, eiF4i and Aurora A were preferentially accumulated in the stratum piramidalis with low staining in the other layers investigated (Fig. 5B,D). In contrast, S6, ZBP1 and CPEB1 staining was more uniformly distributed across the different layers (Fig. 5C,E,F). Subsequently, we measured the effects of a strong neuronal activity, achieved through pilocarpine administration (300 mg/kg body weight). After 3 h of pilocarpine treatment *in vivo*, a significant
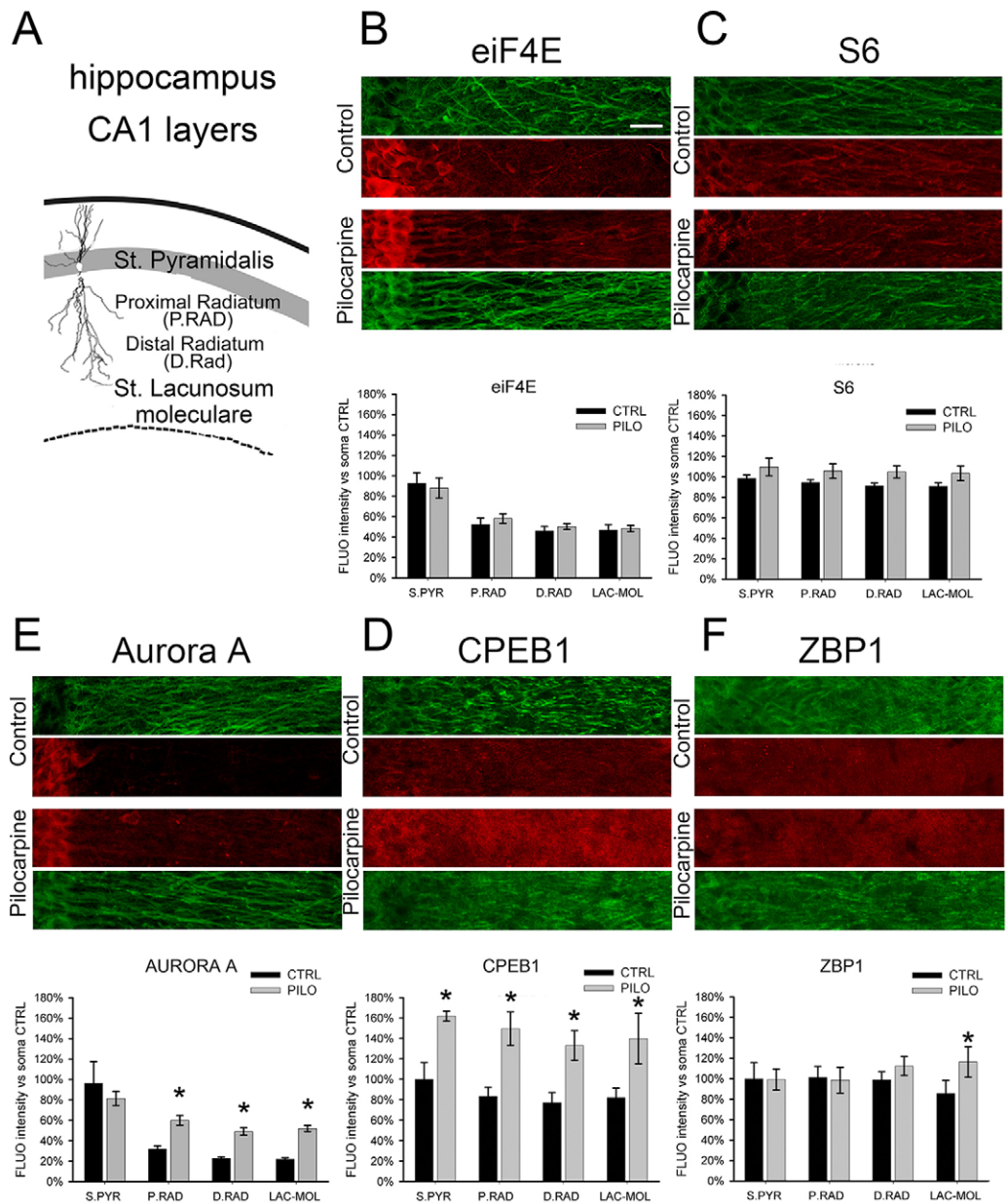
Fig. 5. Translation machinery in CA1 hippocampal laminae upon pilocarpine treatment. (A) Representation of the CA1 hippocampal layers considered in the densitometric quantification of fluorescent staining (upper panels), respectively, for eiF4E (B), S6 (C), Aurora A (E), CPEB1 (D) and ZBP1 (F) (all in red). The slices were all immunostained also for Map2 (green). Bottom panels, quantification of the fluorescence recorded in the different CA1 hippocampal layers, stratum piramidalis (S.Pyr), proximal radiatum (P.Rad), distal radiatum (D.Rad) and lacunosum-moleculare (Lac Mol).The data are mean±s.e.m. normalized to the fluorescence intensity in somatic area of control condition (n=3–5 brain sections). Scale bar: 20 µm. *$P<0.05$ (one-way ANOVA).

increase in CPEB1 fluorescence levels (up to +69±6%; $P<0.05$) could be detected in the stratum piramidalis as well as in the proximal, distal radiatum and stratum lacunosum-moleculare (Fig. 5A,E). Aurora A staining was increased (from +88+4% in proximal radiatum to +136±8% in stratum lacunosum-moleculare, $P<0.05$) particularly in the layers containing the apical dendritic regions (proximal and distal radiatum and stratum lacunosum-moleculare), whereas ZBP1 was upregulated only in the more distal layers (stratum lacunosum-moleculare, +36±15%, $P<0.05$), whereas both proteins were unchanged in the stratum piramidalis of the CA1. The analysis conducted on eiF4E and S6 showed that these elements were not significantly changed following induction of status epilepticus *in vivo*.

DISCUSSION

In a previous study, we provided evidence that KCl induces a marked increase in BDNF levels in dendrites that were mechanically disconnected from the parental soma (Baj et al., 2011). Given that in these conditions BDNF synthesized in the soma could not be delivered to dendrites, we logically concluded that the observed BDNF increase could only be due to a local translation of dendritic mRNA (Baj et al., 2011). In the present study, we assume that even in dendrites that have not been severed from the soma, some of the increased levels of BDNF is due to local translation, although a contribution from somatically produced BDNF cannot be excluded (Lessmann and Brigadski, 2009). Aside from these limitations, using a specific anti-BDNF antibody, we demonstrate that

endogenous BDNF protein synthesis occurs in the entire dendritic arbor, from primary to quaternary branchings. Activity-dependent synthesis of endogenous BDNF is triggered by activation of glutamate and Trk receptors and requires multiple signaling cascades including both global translation regulators such as the RAS–Erk and the mTOR pathways, as well as mRNA-specific regulators such as the CaMKII, Aurora A–CPEB1 and the Src–ZBP1 pathways. We also demonstrated that elements of the translational machinery for these cascades, such as eIF4E, S6 ribosomal protein, Aurora A kinase, CPEB1 and ZBP1, are present both in the soma and dendrites. Neuronal activity enhances the presence in the distal dendritic compartments of mRNA-specific regulators (Aurora A kinase, CPEB1 and ZBP1), whereas the levels of the global regulators (eIF4E and S6) remain unaffected. Importantly, we further show that a chimeric BDNF–GFP transcript 6, which encodes the main dendritic BDNF mRNA, is translated in the same subcellular domains and in response to the same glutamatergic pathways as the endogenous BDNF. As a final point, we confirmed the physiological relevance of these findings by showing *in vivo* that the translational machinery elements investigated are localized and regulated by neuronal activity in the same way as observed in cultured hippocampal neurons.

Detection of endogenous BDNF has proven to be a challenging issue, generating a considerable debate (Edelmann et al., 2014). Therefore, we started by validating the anti-BDNF antibody used in this study taking advantage of hippocampal neurons from transgenic mice in which BDNF is floxed and can be selectively ablated. In BDNF-knockout neurons (i.e. those transfected with cre-recombinase), we were able to obtain specific deletion of BDNF staining, whereas in untransfected neurons anti-BDNF immunoreactivity was clearly detectable, thus demonstrating the specificity of the antibody. We further showed that the antibody was able to recognize the three BDNF forms in western blotting (pro-BDNF, truncated BDNF and mature BDNF). The mature BDNF (14 kDa), is obtained from intracellular or extracellular proteolytic cleavage of the precursor pro-BDNF (32 kDa) (Mowla et al., 2001). However, through a different cleavage, pro-BDNF can equally produce another proteolytic BDNF isoform of 28 kDa called truncated BDNF, which cannot be further cleaved and which has been previously shown to be downregulated in serum and brain of patients with cognitive deficits (Carlino et al., 2011; Garcia et al., 2012; Seidah et al., 1999; Tongiorgi et al., 2012). The literature has provided mixed results regarding the ability of neurons to secrete the different BDNF forms, with a controversy in particular on whether neurons can secrete only mature BDNF or also the proBDNF form (Edelmann et al., 2014; Lessmann and Brigadski, 2009; Matsumoto et al., 2008; Yang et al., 2009). Given that we used total cellular homogenates, our data do not provide information on which BDNF form is secreted. In our previous studies (Baj et al., 2011), we showed an increased BDNF mRNA translation for BDNF and a lasting protein concentration increase in response to KCl stimulation. We are not able to rule out the hypothesis that the strong depolarizing stimuli, used in our assays, might also modify the overall protein stability. However, our immunofluorescence quantification strategy (see Materials and Methods), based on normalizing every signal in the soma and/or dendrites with the parallel staining of the endogenous MAP2 should reduce, if not eliminate, the risk of strong stability variations and subsequent artefact in the measures.

In this study, we used primary cultures of hippocampal neurons at 14 days *in vitro* (DIV 14), whose post-synaptic machinery is known to be functionally mature (Baj et al., 2014; Prange and Murphy, 2001).

Neurons were stimulated with a high-K^+ depolarization solution (50 mM KCl solution), whose positive effects on neurotrophin mRNAs expression levels are well established (Lindholm et al., 1994; Lu et al., 1991; Zafra et al., 1991). Moreover, this highly reproducible model of massive neuronal activity allowed us to overcome the inhibitory signaling that is predominant in lower K^+ culture media (Sala et al., 2005). The timecourse of stimulation (3 h), was based on the Bramham's laboratory studies on Arc synthesis (Messaoudi et al., 2007). This timecourse is also consistent with previous studies from our laboratory, showing an activity-dependent increase on BDNF protein levels after 3 h stimulation *in vitro* and *in vivo* (Tongiorgi et al., 2004, 1997).

The BDNF protein pattern that we observed in dendrites after 3 h depolarization, follows a distribution and timecourse that closely resembles that of its own mRNA (compare this study with Chiaruttini et al., 2009). To further corroborate this observation, we carried out experiments in which we visualized BDNF mRNA and protein produced by an exogenous chimeric construct encoding a BDNF–GFP exon 6 transcript at the same time. This transcript was found to be mainly localized in dendrites (Baj et al., 2013) and to be poorly translatable in absence of neuronal activation (Vaghi et al., 2014). Using a similar construct, we have previously shown that the local protein synthesis of BDNF can occur in dendrites even when they are mechanically severed from the soma (Baj et al., 2011). Accordingly, we demonstrated here, that depolarization induces a strong increase in dendritic localization of both mRNA and protein with no measurable changes in the soma. Taken together, these experiments represent further evidence that BDNF can be locally translated in dendrites. However, in resting cultures, the distribution of BDNF mRNA in dendrites is generally more proximal than that of the BDNF protein (An et al., 2008; Baj et al., 2011; Chiaruttini et al., 2009; Tongiorgi, 2008). Thus, we cannot exclude that the remarkable BDNF signal visible up to the fourth order dendrites even in resting cultures, could be at least in part due to BDNF protein transport from the soma. Previous studies have shown that BDNF protein is transported from the soma to dendrites in vesicles generated from the Golgi complex resident in the somata (Brigadski et al., 2005; Dieni et al., 2012; Kuczewski et al., 2009; Lessmann and Brigadski, 2009; Tongiorgi and Baj, 2008). It is worth noting here, that the absence of a depolarization-induced increased BDNF expression in the soma could be masked by the already strong basal expression. In conclusion, it remains to be determined whether the BDNF synthesized in dendrites has additive or different functions, and same or different release sites, with respect to somatic BDNF.

The mechanisms leading to activation of the post-synaptic translational machinery responsible for local protein synthesis in dendrites are still poorly understood. To determine how dendritic BDNF translation is regulated, we considered the main post-synaptic pathways activated by glutamate (Bramham and Wells, 2007; Panja and Bramham, 2014). The signaling cascades involved were dissected out by analyzing five major players of mRNA circularization and translation. It is interesting that each inhibitor, in our experimental conditions, produces an all or nothing response. This suggests that BDNF translation is very strictly controlled and that several aspects of translational control need to work in combination to allow BDNF production. In addition, we investigated the distribution pattern in resting and stimulated conditions, of the cap-dependent eIF4E, the ribosomal protein S6 (S6), Aurora kinase A and the RBPs ZBP1 and CPEB1. This approach was aimed at investigating their possible involvement on BDNF translational regulation as well as their localization in neuronal compartments.

Initiation is considered the major rate-limiting step of translational regulation during which mRNA and ribosome start their interaction and cap-dependent initiation factors are recruited (Gal-Ben-Ari et al., 2012; Santini and Klann, 2014). We investigated eiF4E because it is the main limiting factor of the cap-dependent initiation. As predicted, specific eiF4E immunostaining was preferentially detected in the somata (Lang et al., 1994; Lejbkowicz et al., 1992), although its presence in dendritic distal portions was also visible and remained constant in all the subcellular domains even after neuronal activity induced by KCl or pilocarpine seizures. Previous studies have reported the presence of eiF4E immunoreactivity at postsynaptic sites, especially in structures underneath the postsynaptic membrane in the spine, some of which are in close proximity to post-synaptic densities (Asaki et al., 2003).

It has been previously established that mRNA transport to dendrites is achieved through the formation of RNA granules, some of which contain ribosomes aggregated with mRNAs (Kanai et al., 2004; Knowles et al., 1996; Krichevsky and Kosik, 2001; Tang et al., 2001). In particular, it has been shown that mRNA–ribosome complexes can be transported in dendrites as transporting granules in which translation is repressed and, therefore, ribosomal proteins, such as the S6 protein that we studied here, are considered good biomarkers of dendritic mRNA granules (Graber et al., 2013; Kim et al., 2005; Sossin and DesGroseillers, 2006). In addition, the level of the ribosomal protein S6 is a good marker of the amount of ribosome and an indicator of the translational potential within neurons (Costa-Mattioli et al., 2009). We found that S6 protein is equally distributed between soma and dendrites and that its level did not change upon electrical activity. This is a very new finding, which suggests that ribosomes are not in limiting numbers in dendrites. In conclusion, we present data concerning the global regulators of translation eiF4E and S6 ribosomal protein and we show that their levels are not affected by electrical stimulation *in vitro* and *in vivo*.

RBPs such as ZBP1 and CPEB1 are now emerging as possible specific regulators of translation, because of their ability to interact with specific sequences in the 3′UTR of a selected group of mRNAs. The best known example is the polyadenylation-dependent translation of CaMKIIα whose CPEB1-mediated translational repression can be relieved though phosphorylation of CPEB1 by either by Aurora A kinase (Huang et al., 2002; Wells et al., 2001) or CaMKIIα itself (Atkins et al., 2004). Our densitometric analyses on cultured hippocampal neurons and in hippocampus CA1 *in vivo*, shows that Aurora A is mostly located in the somatic area in resting neurons, but after 3 h of stimulation, it can be detected at great distances in dendrites suggesting a key role of this kinase in dendrites. Aurora-A-dependent translation of BDNF is possible thanks to the presence of CPE-containing sequences in the 3′UTR of BDNF mRNAs and the demonstrated binding of CPEB1 to it (Oe and Yoneda, 2010). CPEB1 itself is strongly accumulated along the entire dendritic arbor in response to activity both *in vitro* and *in vivo*, in agreement with a role of this pathway in regulating BDNF translation in dendrites. Interestingly, in our hands, ZBP1 immunofluorescence is upregulated by activity in the most distal dendritic compartments, that is, from the secondary branching points onward. ZBP1 has been shown to bind to β-actin mRNA in fibroblasts and neurons where it plays a role in mRNA trafficking (Tiruchinapalli et al., 2003), but it has also been shown to play a role in translation. During mRNA trafficking, ZBP1 represses β-actin translation, but its phosphorylation by Src kinase results in the release of β-actin mRNA from ZBP1-containing granules and its local translation (Hüttelmaier et al., 2005). A putative ZBP1 cis-element is present in BDNF mRNA (data not shown) but a direct association between ZBP1 and BDNF mRNA has not been proven yet. In conclusion, these data suggest that BDNF translation in dendrites is controlled by multiple RBPs, which are also involved in its transport in dendrites. It is remarkable that the very same proteins that are responsible for the translational repression occurring during mRNA traveling in dendrites, are also involved in translational activation in response to specific signaling cascades.

In conclusion, in this study, we describe the compartment and the signaling cascades required for local BDNF translation in dendrites in response to excitatory inputs that are known to be involved in long-term plasticity mechanisms. These results add up to previous evidence demonstrating that, in addition to transported BDNF from soma, synthesis of this neurotrophic factor can occur in dendrites.

MATERIALS AND METHODS
Cell cultures and transfection
Animal use was approved by the Italian Ministry of Health under authorization no. 185/2010-B. Primary hippocampal neurons were prepared from postnatal day 1 Wistar rats as described by Aibel (Aibel et al., 1998), with minor modifications. Cells were plated on coverslips coated with 2% Matrigel (BD Biosciences) in 24-well plates at a density of 2×10^5 cells/ml per well and cultured in a 5% CO_2 humidified incubator in Neurobasal medium (Life Technologies) supplemented with B27 (Life Technologies), 1 mM L-glutamine (Euroclone), and antibiotics (Euroclone). The medium was changed every 2 days from the second day in culture onward. Neuron transfection was performed using Lipofectamine 2000 (Life Technologies) following the manufacturer's instructions. Specifically, for the results presented in Fig. 1A we co-transfected pEGFP-N1 (Clontech) and CRE-recombinase-expressing vectors (1 µg each) (kindly provided by Andrès Muro, ICGEB, Trieste, Italy) in hippocampal neurons from BDNF[lox/lox] transgenic mice (The Jackson Laboratory, Bar Harbor, ME, USA) at DIV6 and fixed at DIV12. The pExon6-BDNF-GFP-3′UTR-long vector was as previously described (Baj et al., 2011) In all experiments, the transfection mix was removed after 1 h and for *in situ* hybridization and the luciferase assay cells were blocked at 24 h after transfection.

Cell treatment
Hippocampal neurons (HpN) at DIV14 were treated with a high-K^+ concentration physiological solution (50 mM KCl, 1.8 mM $CaCl_2$, 0.8 mM $MgSO_4$, 101 mM NaCl, 26 mM $NaHCO_3$, 1 mM NaH_2PO_4, 0.7% D-glucose, 15 mM HEPES, pH 7.4) (all from Sigma-Aldrich) for 3 h. Hippocampal neurons were left in complete neurobasal medium for control experiments. Specific translational blockade experiments were performed by pre-treating neurons 30 min in advance with the following pharmacological inhibitor: cycloheximide (50 µg/ml), extracellular blocker:DNQX (20 µM), kinurenic acid (2 mM), K252a (467 nM), U0126 (50 µM) (Cavanaugh et al., 2001; Kanhema et al., 2006), rapamycin (20 nM) (Beretta et al., 1996; Takei et al., 2004, 2001; Tang et al., 2002); GF (50 nM) (Heikkila et al., 1993). KN62 (20 µM) (Hidaka and Yokokura, 1996), PP2 (20 µM) (Perkinton et al., 1999), UO124 (50 µM), SU5402 (50 µM), SB505124 (5 µM) (all from Sigma-Aldrich) and Aurora A inhibitor (PHA-680632, 10 µM) (Soncini et al., 2006). PHA-680632 was kindly provided by Nerviano Medical Sciences (Nerviano, Milano, Italy).

Immunofluorescence
After treatment, coverslips containing 14DIV hippocampal neurons were washed in PBS and fixed in a 2% paraformaldehyde (PFA) solution for 15 min. Cells were permeabilized with PBS 0.5% Triton X-100 for 15 min and blocked with PBS containing 2% bovine serum albumin (BSA) for 30 min. The following primary antibodies were diluted in blocking solution and incubated overnight at 4°C: rabbit anti-Aurora A (AIK) 1:200 [Cell Signaling, cat. 3092; specifity shown in Polacchini et al. (2016) and Fig. S1D], mouse anti-BDNF 1:50 (Sigma-Aldrich, cat. B5050), rabbit anti-eiF4E 1:200 (Sigma-Aldrich, cat. B5906; Dostie et al., 2000), goat anti-ribosomal protein S6 1:200 (Santa Cruz Biotechnology, cat. sc13007;

Kodiha et al., 2005), rabbit anti-MAP2 1:200 (Santa Cruz Biotechnology, cat. sc20172), mouse anti-MAP2 1:200 (Sigma-Aldrich, cat. M1406), rabbit anti-CPEB1 1:200 (Abcam, cat. AB73287; Vicario et al., 2015) and rabbit anti-ZBP1 1:200 (IGF2BP1, Abcam, cat. AB82968; Song et al., 2013). After a 3× rinse in PBS, the respective conjugates (all diluted 1:200 in PBS) were incubated for 2 h at room temperature: goat anti-rabbit-IgG conjugated to Alexa Fluor 488 (Life Technologies A11008 for Aurora kinase A, eiF4E, CPEB1, ZBP1 and MAP2), goat anti-mouse-IgG conjugated to Alexa Fluor 568 (Life Technologies A11004 for BDNF and MAP2), donkey anti-goat-IgG conjugated to Alexa Fluor 568 (Life Technologies A11057 for ribosomal protein S6) and goat anti-mouse-IgG conjugated to Alexa Fluor 488 (Life Technologies A11001 for MAP2). Finally, the cell nuclei were stained by incubating the coverslips with Hoescht 33258 (Sigma-Aldrich, cat. B2883) at 1:1000 in PBS (10 ng/ml) for 10 min at room temperature and the slides were closed using an anti-fade mountant (Mowiol® 40-88, Sigma-Aldrich). Of note, in each experiment, we subdivided neurons extracted from pooled hippocampi on different coverslips which then contained virtually the same neurons and, therefore, results are comparable across the different coverslips. Immunofluorescence was carried out simultaneously within a 24-well plate containing all the coverslips from one neuronal culture. This ensures that immunostaining can provide comparable results. Each immunofluorescence signal within one culture was normalized to its own internal control represented by the immunofluorescence values of neuronal somata measured on two untreated coverlips, whose average value is used as 100% for that culture. Given that every single individual culture is normalized to 100%, every culture will have data expressed in the same, perfectly comparable manner.

Fluorescence *in situ* hybridization

The riboprobe for GFP was generated from a coding sequence fragment excised from the commercial vector pEGFP-N1 (restriction sites BamHI and NotI) and cloned into pBLKS II vector (Fermentas, Life Technologies). The template vector was used in conjunction with T7 RNA pol and Dig-RNA labeling mix (Roche) to produce the antisense probe. The *in situ* hybridization was performed as previously described (Tongiorgi et al., 1997, 1998) with slight modifications.

The permeabilization and hybrization steps produced a strong bleaching of the native GFP fluorescence; consequently, we retrieved the signal from BDNF–GFP chimeric proteins by performing an immunostaining against GFP. A mouse monoclonal anti-Dig antibody (1:500, cat. no. 11333062910, Roche) was used in parallel with a rabbit polyclonal anti-GFP antibody (1:250, cat. no. sc-8334, Santa Cruz Biotechnology). Staining for GFP RNA and protein were achieved respectively with the secondary antibodies anti-rabbit-IgG conjugated to Alexa Fluor 568 and anti-mouse-IgG conjugated to Alexa Fluor 488.

Construction of luciferase vectors and translation assay

The luciferase constructs and translation assay presented in Fig. 4 were as previously described (Vaghi et al., 2014). In brief, firefly and *Renilla* luciferase coding sequences were subcloned respectively from pGL3 (U47295) and pRL (AF025845) vectors (Promega) and inserted into the AgeI and NotI in pEGFP-N1 (U55762, Clontech) following excision of GFP sequence. The two luciferase reporter genes are under the control of CMV promoter. The specific BDNF 5′UTR (exon 6, EF125680) and 3′UTR (EF125675) were respectively inserted into the XhoI/AgeI and NotI/HpaI sites of the firefly-luciferase-generated vector. Firefly luciferase and *Renilla* luciferase vector were co-transfected at a 10:1 ratio (2 µg total). Transfected cells (two wells of a 24-multiwell plate) were washed and directly harvested and homogenized in the lysis buffer (Promega). The activity was measured with the dual-luciferase reporter assay system (Promega) using a Luminometer (GloMax, Promega). Luciferase readings were taken as singlets. Ratios of *Renilla* luciferase readings to firefly luciferase readings were taken for each experiment and duplicates were averaged. The values were normalized to the activity of the empty construct (Firefly luciferase on *Renilla* luciferase) in case of basal translatability. The treatments were normalized to the activity of the target construct (5′UTR-FLuc-3′UTR on *Renilla* luciferase) in control conditions. Luciferase activities are expressed as the mean±s.e.m. from three independent experiments.

Animal treatments and immunohistochemistry

The animals were maintained with ad libidum access to food and water under standard conditions: 22°C (±1°C), 50% relative humidity, and a 12-h-light–12-h-dark cycle. For immunohistochemical experiments adult male Sprague-Dawley rats were injected intra-peritoneally (i.p.) with 300 mg/kg body weight pilocarpine for 3 h under urethane (Sigma-Aldrich) anaesthesia (1 g/kg body weight i.p.). Control animals were treated with a physiological solution containing 0.9% NaCl. Rats were placed under terminal anesthesia and transcardially perfused with ice-cold 4% PFA in PBS (pH 7.4). The brains were extracted, post-fixed in PFA for ~4 h and afterwards cryopreserved in 20% sucrose (Sigma-Aldrich) in PBS. Brains were quickly frozen with CO_2 and cut in serial 40-µm thick coronal sections with the Histoslide 200R cryomicrotome (Leica). Free-floating slices were washed 3×5 min in Tris-buffered saline (TBS; Tris-HCl 0.1 M, NaCl 0.5 M, pH 7.4); then blocked in Tris-X solution (TBS with 0.3% Triton X-100 and 0.75% BSA) for 1 h; and finally they were incubated overnight with the same antibodies used for immunocitochemistry. Afterwards, slices were put at room temperature for 4 h, washed for 5 min three times in Tris-X solution, and finally incubated with the respective Alexa Fluor conjugates (all diluted 1:200 in Tris-X solution) for 2 h. Slices were then washed 5 min three times in Tris-Y solution (TBS with 0.3% Triton X-100 and 0.25% BSA). Finally, the nucleus was stained by incubating with 1:1000 Hoescht 33258 for 10 min at room temperature. After that, slices were again rinsed and finally mounted on gelatinized slides using the fluorescence anti-fade mountant. All passages were performed in gentle shaking.

Data acquisition and analysis

Immunofluorescence experiments were evaluated with a Nikon C1si confocal microscope (Nikon, Tokyo, Japan), containing a 488-nm argon laser and 561-nm diode lasers. Light was delivered to the sample with an 80/20 reflector. The system was operated with a pinhole size of one Airy disk (30 nm). Electronic zoom was kept at minimum values for measurements to reduce potential bleaching. 60× Plan Apo objectives were used, collecting a series of optical images at 0.15 µm z-resolution step sizes. Images were processed for z-projection by using ImageJ 1.43 m (NIH, Bethesda, USA). Quantitative data were collected on all optical slices describing the selected subcellular structure and normalized for the MAP2 staining stack by stack. The specific neuronal area was measured using the MAP2 staining of soma, dendrites and branch points. A common constant threshold was applied to generate a mask of positive pixels, showing the neuronal morphology. The staining quantification was performed on defined subcellular regions (Fig. 1D) and analyzed by the ImageJ tool regions of interest (ROI) manager. The staining intensity in the soma was measured using a circular area with a diameter of ~10–15 µm. Primary dendrite staining (D1) was defined with a polygonal ROI (~25×10 µm²) drawn within the first 50 µm from the somatic area. The first branch point (BP1), defined as the first intersection point between primary and secondary dendrites, typically at 30–70 µm from the soma, was measured within a circular ROI with ~8 µm diameter. The secondary dendrite (D2), described as the dendritic part (with a 2.5–5 µm diameter) between the first and second branch points, usually at 40–100 µm from the soma, was measured in a polygonal ROI (~20×8 µm). The staining intensity in the second branch point (BP2), defined as the intersection point between secondary and tertiary dendrites, generally at 50–100 µm from the soma, was quantified in a circular ROI of ~5 µm. Tertiary and quaternary dendrites (D3&4), dendritic structures with ~2 µm diameter present after the second branch points and up to 100 µm from the somatic area, were here drawn as a polygonal ROIs of ~20×4 µm. The third and forth branch points (BP3&4), intersection points located after the second branch point and up to 7 µm from the soma, were selected as a circular ROIs with a diameter ~2–3 µm, and intersection points located after the second branch point and up to 7 µm from the soma were selected as circular ROIs with a diameter ~2–3 µm. The detector gain was adjusted for each image in order to record the background signal, taken outside the neurons, at the same level of the noise signal. The noise signal is an intrinsic property of the photomultiplier and for the Nikon C1Si was found to be at the intensity level of 40–50 on the available 4096 intensity levels (12-bit). The signal intensity for each target protein (BDNF, S6, eiF4E, AuA, CPEB1 or ZBP1) was recorded and divided, stack by stack, with the signal for MAP2 coming from

the corresponding channel. This ratio value is represented our densitometry measurements. This approach allowed us to compensate for possible fluorescence variations due to different efficiency of the immunostaining or to different fluorophore quantum yield at the moment of picture gathering. In brief, dividing each signal with its own MAP2 signal permitted an endogenous normalization of the intensity levels.

Finally, the densitometry data were normalized to the value recorded in soma of control cells in order to describe both the relative protein distribution from soma to dendritic regions and the variations from control to stimulated conditions. Quantitative analysis refers to at least three different experiments in which about 100 measures per condition were made.

Western blotting and ELISA

Hippocampal neurons were plated at high density on a mw6 plate (500,000 cells/plate) and maintained in culture. The cells were stimulated at DIV14 with control solution or with KCl (50 mM final concentration) for 3 h, respectively. Hippocampal neurons were lysed in 137 mM NaCl, 20 mM Tris-HCl pH 8.0,1% NP40, 10% glycerol, 1 mM PMSF,10 μg/ml aprotinin, 1 μg/ml leupeptin and 0.5 mM sodium vanadate and stored at −80°. The cell lysates were centrifuged (13,000 g, 4° C, 15 min). Pellet fractions of the cell lysates were loaded for the subsequent western blot analysis. Control immunostaining for α-tubulin (Sigma-Aldrich) was performed with primary antibody at 1:200 and secondary antibody at 1:10,000 all in PBS with 0.1% (v/v) Tween-20 (PBST) with 2% milk, and specific immunostaining for BDNF protein isoforms (Sigma-Aldrich) was performed primary antibody at 1:200 and secondary antibody at 1:5000 all in PBST with 2% milk. The immunoreactive bands were detected using the X-ray films (Kodak) and ECL reagent (Amersham, Pittsburgh, PA) and following the manufacturer's instructions. Western blot data refers to at least three different experiments, all quantified by the Quantity One® 4.6.6. software (Bio-Rad). The BDNF endogenous quantification was achieved through ELISA techniques performed using a BDNF Emax immunoassay system (Promega) following the manufacturer's instructions and a compatible microplate reader.

Data representation and statistical methods

Bar graphs are represented the mean±s.e.m. of all measurements (see Results). Possible outliners were analyzed by the GraphPad Software (GraphPad Inc, La Jolla, CA, USA) online resource 'Outlier calculator', using the standard 0.05 alpha value (http://www.graphpad.com/quickcalcs/). All the statistical data analysis was performed with the Sigma Plot 11 software (Systat Software, Inc., San Jose, CA). Statistical significance among groups was evaluated performing one-way ANOVA with Holm-Sidak's method and $P<0.05$ was considered significant.

References
Aibel, L., Martin-Zanca, D., Perez, P. and Chao, M. V. (1998). Functional expression of TrkA receptors in hippocampal neurons. *J. Neurosci. Res.* **54**, 424-431.

Aid, T., Kazantseva, A., Piirsoo, M., Palm, K. and Timmusk, T. (2007). Mouse and ratBDNF gene structure and expression revisited. *J. Neurosci. Res.* **85**, 525-535.

An, J. J., Gharami, K., Liao, G.-Y., Woo, N. H., Lau, A. G., Vanevski, F., Torre, E. R., Jones, K. R., Feng, Y., Lu, B. et al. (2008). Distinct role of long 3′ UTR BDNF mRNA in spine morphology and synaptic plasticity in hippocampal neurons. *Cell* **134**, 175-187.

Asaki, C., Usuda, N., Nakazawa, A., Kametani, K. and Suzuki, T. (2003). Localization of translational components at the ultramicroscopic level at postsynaptic sites of the rat brain. *Brain Res.* **972**, 168-176.

Atkins, C. M., Nozaki, N., Shigeri, Y. and Soderling, T. R. (2004). Cytoplasmic polyadenylation element binding protein-dependent protein synthesis is regulated by calcium/calmodulin-dependent protein kinase II. *J. Neurosci.* **24**, 5193-5201.

Baj, G., Leone, E., Chao, M. V. and Tongiorgi, E. (2011). Spatial segregation of BDNF transcripts enables BDNF to differentially shape distinct dendritic compartments. *Proc. Natl. Acad. Sci. USA* **108**, 16813-16818.

Baj, G., D'Alessandro, V., Musazzi, L., Mallei, A., Sartori, C. R., Sciancalepore, M., Tardito, D., Langone, F., Popoli, M. and Tongiorgi, E. (2012). Physical exercise and antidepressants enhance BDNF targeting in hippocampal CA3 dendrites: further evidence of a spatial code for BDNF splice variants. *Neuropsychopharmacology* **37**, 1600-1611.

Baj, G., Del Turco, D., Schlaudraff, J., Torelli, L., Deller, T. and Tongiorgi, E. (2013). Regulation of the spatial code for BDNF mRNA isoforms in the rat hippocampus following pilocarpine-treatment: a systematic analysis using laser microdissection and quantitative real-time PCR. *Hippocampus* **23**, 413-423.

Baj, G., Patrizio, A., Montalbano, A., Sciancalepore, M. and Tongiorgi, E. (2014). Developmental and maintenance defects in Rett syndrome neurons identified by a new mouse staging system in vitro. *Front. Cell Neurosci.* **8**, 18.

Beretta, L., Gingras, A. C., Svitkin, Y. V., Hall, M. N. and Sonenberg, N. (1996). Rapamycin blocks the phosphorylation of 4E-BP1 and inhibits cap-dependent initiation of translation. *EMBO J.* **15**, 658-664.

Bramham, C. R. and Wells, D. G. (2007). Dendritic mRNA: transport, translation and function. *Nat. Rev. Neurosci.* **8**, 776-789.

Brigadski, T., Hartmann, M. and Lessmann, V. (2005). Differential vesicular targeting and time course of synaptic secretion of the mammalian neurotrophins. *J. Neurosci.* **25**, 7601-7614.

Cáceres, A., Ye, B. and Dotti, C. G. (2012). Neuronal polarity: demarcation, growth and commitment. *Curr. Opin. Cell Biol.* **24**, 547-553.

Carlino, D., Leone, E., Di Cola, F., Baj, G., Marin, R., Dinelli, G., Tongiorgi, E. and De Vanna, M. (2011). Low serum truncated-BDNF isoform correlates with higher cognitive impairment in schizophrenia. *J. Psychiatr. Res.* **45**, 273-279.

Cavanaugh, J. E., Ham, J., Hetman, M., Poser, S., Yan, C. and Xia, Z. (2001). Differential regulation of mitogen-activated protein kinases ERK1/2 and ERK5 by neurotrophins, neuronal activity, and cAMP in neurons. *J. Neurosci.* **21**, 434-443.

Chiaruttini, C., Vicario, A., Li, Z., Baj, G., Braiuca, P., Wu, Y., Lee, F. S., Gardossi, L., Baraban, J. M. and Tongiorgi, E. (2009). Dendritic trafficking of BDNF mRNA is mediated by translin and blocked by the G196A (Val66Met) mutation. *Proc. Natl. Acad. Sci. USA* **106**, 16481-16486.

Costa-Mattioli, M., Sossin, W. S., Klann, E. and Sonenberg, N. (2009). Translational control of long-lasting synaptic plasticity and memory. *Neuron* **61**, 10-26.

Dieni, S., Matsumoto, T., Dekkers, M., Rauskolb, S., Ionescu, M. S., Deogracias, R., Gundelfinger, E. D., Kojima, M., Nestel, S., Frotscher, M. et al. (2012). BDNF and its pro-peptide are stored in presynaptic dense core vesicles in brain neurons. *J. Cell Biol.* **196**, 775-788.

Dostie, J., Lejbkowicz, F. and Sonenberg, N. (2000). Nuclear eukaryotic initiation factor 4E (eIF4E) colocalizes with splicing factors in speckles. *J. Cell Biol.* **148**, 239-246.

Edelmann, E., Lessmann, V. and Brigadski, T. (2014). Pre- and postsynaptic twists in BDNF secretion and action in synaptic plasticity. *Neuropharmacology* **76**, 610-627.

Fiala, J. C., Spacek, J. and Harris, K. M. (2007). Dendrite structure. Chapter 1, pp. 1-41, In *Dendrites* (ed. O. U. press). Oxford University press.

Gal-Ben-Ari, S., Kenney, J. W., Ounalla-Saad, H., Taha, E., David, O., Levitan, D., Gildish, I., Panja, D., Pai, B., Wibrand, K. et al. (2012). Consolidation and translation regulation. *Learn. Mem.* **19**, 410-422.

Garcia, K. L. P., Yu, G., Nicolini, C., Michalski, B., Garzon, D. J., Chiu, V. S., Tongiorgi, E., Szatmari, P. and Fahnestock, M. (2012). Altered balance of proteolytic isoforms of pro-brain-derived neurotrophic factor in autism. *J. Neuropathol. Exp. Neurol.* **71**, 289-297.

Gorski, J. A., Zeiler, S. R., Tamowski, S. and Jones, K. R. (2003). Brain-derived neurotrophic factor is required for the maintenance of cortical dendrites. *J. Neurosci.* **23**, 6856-6865.

Graber, T. E., Hebert-Seropian, S., Khoutorsky, A., David, A., Yewdell, J. W., Lacaille, J.-C. and Sossin, W. S. (2013). Reactivation of stalled polyribosomes in synaptic plasticity. *Proc. Natl. Acad. Sci. USA* **110**, 16205-16210.

Heikkila, J., Jalava, A. and Eriksson, K. (1993). The selective protein kinase C inhibitor GF 109203X inhibits phorbol ester-induced morphological and functional differentiation of SH-SY5Y human neuroblastoma cells. *Biochem. Biophys. Res. Commun.* **197**, 1185-1193.

Hidaka, H. and Yokokura, H. (1996). Molecular and cellular pharmacology of a calcium -dependent protein kinase II (CaM kinase II) inhibitor, KN-62, and proposal of CaM kinase phosphorylation cascades. *Adv. Pharmacol.* **36**, 193-219.

Huang, Y.-S., Jung, M. Y., Sarkissian, M. and Richter, J. D. (2002). N-methyl-D-aspartate receptor signaling results in Aurora kinase-catalyzed CPEB phosphorylation and alphaCaMKII mRNA polyadenylation at synapses. *EMBO J.* **21**, 2139-2148.

Hüttelmaier, S., Zenklusen, D., Lederer, M., Dictenberg, J., Lorenz, M., Meng, X., Bassell, G. J., Condeelis, J. and Singer, R. H. (2005). Spatial regulation of beta-actin translation by Src-dependent phosphorylation of ZBP1. *Nature* **438**, 512-515.

Kanai, Y., Dohmae, N. and Hirokawa, N. (2004). Kinesin transports RNA: isolation and characterization of an RNA-transporting granule. *Neuron* **43**, 513-525.

Kanhema, T., Dagestad, G., Panja, D., Tiron, A., Messaoudi, E., Håvik, B., Ying, S.-W., Nairn, A. C., Sonenberg, N. and Bramham, C. R. (2006). Dual regulation of translation initiation and peptide chain elongation during BDNF-induced LTP in vivo: evidence for compartment-specific translation control. *J. Neurochem.* **99**, 1328-1337.

Kellner, Y., Gödecke, N., Dierkes, T., Thieme, N., Zagrebelsky, M. and Korte, M. (2014). The BDNF effects on dendritic spines of mature hippocampal neurons depend on neuronal activity. *Front. Synaptic Neurosci.* **6**, 5.

Kim, H. K., Kim, Y.-B., Kim, E.-G. and Schuman, E. (2005). Measurement of dendritic mRNA transport using ribosomal markers. *Biochem. Biophys. Res. Commun.* **328**, 895-900.

Knowles, R. B., Sabry, J. H., Martone, M. E., Deerinck, T. J., Ellisman, M. H., Bassell, G. J. and Kosik, K. S. (1996). Translocation of RNA granules in living neurons. *J. Neurosci.* **16**, 7812-7820.

Kodiha, M., Chu, A., Lazrak, O. and Stochaj, U. (2005). Stress inhibits nucleocytoplasmic shuttling of heat shock protein hsc70. *Am. J. Physiol. Cell Physiol.* **289**, C1034-C1041.

Krichevsky, A. M. and Kosik, K. S. (2001). Neuronal RNA granules: a link between RNA localization and stimulation-dependent translation. *Neuron* **32**, 683-696.

Kuczewski, N., Porcher, C., Lessmann, V., Medina, I. and Gaiarsa, J. L. (2009). Activity-dependent dendritic release of BDNF and biological consequences. *Mol. Neurobiol.* **39**, 37-49.

Lang, V., Zanchin, N. I., Lunsdorf, H., Tuite, M. and McCarthy, J. E. (1994). Initiation factor eIF-4E of Saccharomyces cerevisiae. Distribution within the cell, binding to mRNA, and consequences of its overproduction. *J. Biol. Chem.* **269**, 6117-6123.

Leal, G., Comprido, D. and Duarte, C. B. (2014). BDNF-induced local protein synthesis and synaptic plasticity. *Neuropharmacology* **76**, 639-656.

Lejbkowicz, F., Goyer, C., Darveau, A., Neron, S., Lemieux, R. and Sonenberg, N. (1992). A fraction of the mRNA 5′ cap-binding protein, eukaryotic initiation factor 4E, localizes to the nucleus. *Proc. Natl. Acad. Sci. USA* **89**, 9612-9616.

Lessmann, V. and Brigadski, T. (2009). Mechanisms, locations, and kinetics of synaptic BDNF secretion: an update. *Neurosci. Res.* **65**, 11-22.

Lim, C. S. and Alkon, D. L. (2012). Protein kinase C stimulates HuD-mediated mRNA stability and protein expression of neurotrophic factors and enhances dendritic maturation of hippocampal neurons in culture. *Hippocampus* **22**, 2303-2319.

Lindholm, D., Castrén, E., Berzaghi, M., Blöchl, A. and Thoenen, H. (1994). Activity-dependent and hormonal regulation of neurotrophin mRNA levels in brain-implications for neuronal plasticity. *J. Neurobiol.* **25**, 1362-1372.

Lu, B., Yokoyama, M., Dreyfus, C. F. and Black, I. B. (1991). Depolarizing stimuli regulate nerve growth factor gene expression in cultured hippocampal neurons. *Proc. Natl. Acad. Sci. USA* **88**, 6289-6292.

Matsumoto, T., Rauskolb, S., Polack, M., Klose, J., Kolbeck, R., Korte, M. and Barde, Y.-A. (2008). Biosynthesis and processing of endogenous BDNF: CNS neurons store and secrete BDNF, not pro-BDNF. *Nat. Neurosci.* **11**, 131-133.

Megías, M., Emri, Z., Freund, T. F. and Gulyas, A. I. (2001). Total number and distribution of inhibitory and excitatory synapses on hippocampal CA1 pyramidal cells. *Neuroscience* **102**, 527-540.

Messaoudi, E., Kanhema, T., Soule, J., Tiron, A., Dagyte, G., da Silva, B. and Bramham, C. R. (2007). Sustained Arc/Arg3.1 synthesis controls long-term potentiation consolidation through regulation of local actin polymerization in the dentate gyrus in vivo. *J. Neurosci.* **27**, 10445-10455.

Mowla, S. J., Farhadi, H. F., Pareek, S., Atwal, J. K., Morris, S. J., Seidah, N. G. and Murphy, R. A. (2001). Biosynthesis and post-translational processing of the precursor to brain-derived neurotrophic factor. *J. Biol. Chem.* **276**, 12660-12666.

Oe, S. and Yoneda, Y. (2010). Cytoplasmic polyadenylation element-like sequences are involved in dendritic targeting of BDNF mRNA in hippocampal neurons. *FEBS Lett.* **584**, 3424-3430.

Panja, D. and Bramham, C. R. (2014). BDNF mechanisms in late LTP formation: a synthesis and breakdown. *Neuropharmacology* **76**, 664-676.

Perkinton, M. S., Sihra, T. S. and Williams, R. J. (1999). Ca(2+)-permeable AMPA receptors induce phosphorylation of cAMP response element-binding protein through a phosphatidylinositol 3-kinase-dependent stimulation of the mitogen-activated protein kinase signaling cascade in neurons. *J. Neurosci.* **19**, 5861-5874.

Polacchini, A., Albani, C., Baj, G., Colliva, A., Carpinelli, P., Tongiorgi, E. (2016). Combined cisplatin and aurora inhibitor treatment increase neuroblastoma cell death but surviving cells overproduce BDNF. *Biol Open*. doi:10.1242/bio.016725. [Epub].

Polacchini, A., Metelli, G., Francavilla, R., Baj, G., Florean, M., Mascaretti, L. G. and Tongiorgi, E. (2015). A method for reproducible measurements of serum BDNF: comparison of the performance of six commercial assays. *Sci. Rep.* **5**, 17989.

Prange, O. and Murphy, T. H. (2001). Modular transport of postsynaptic density-95 clusters and association with stable spine precursors during early development of cortical neurons. *J. Neurosci.* **21**, 9325-9333.

Richter, J. D. and Klann, E. (2009). Making synaptic plasticity and memory last: mechanisms of translational regulation. *Genes Dev.* **23**, 1-11.

Sala, C., Roussignol, G., Meldolesi, J. and Fagni, L. (2005). Key role of the postsynaptic density scaffold proteins Shank and Homer in the functional architecture of Ca2+ homeostasis at dendritic spines in hippocampal neurons. *J. Neurosci.* **25**, 4587-4592.

Santini, E. and Klann, E. (2014). Reciprocal signaling between translational control pathways and synaptic proteins in autism spectrum disorders. *Sci. Signal.* **7**, re10.

Seidah, N. G., Mowla, S. J., Hamelin, J., Mamarbachi, A. M., Benjannet, S., Toure, B. B., Basak, A., Munzer, J. S., Marcinkiewicz, J., Zhong, M. et al. (1999). Mammalian subtilisin/kexin isozyme SKI-1: a widely expressed proprotein convertase with a unique cleavage specificity and cellular localization. *Proc. Natl. Acad. Sci. USA* **96**, 1321-1326.

Soncini, C., Carpinelli, P., Gianellini, L., Fancelli, D., Vianello, P., Rusconi, L., Storici, P., Zugnoni, P., Pesenti, E., Croci, V. et al. (2006). PHA-680632, a novel Aurora kinase inhibitor with potent antitumoral activity. *Clin. Cancer Res.* **12**, 4080-4089.

Song, J. S., Hwang, D. H., Kim, S.-O., Jeon, M., Choi, B.-J., Jung, H.-S., Moon, S. J., Park, W. and Choi, H.-J. (2013). Comparative gene expression analysis of the human periodontal ligament in deciduous and permanent teeth. *PLoS ONE* **8**, e61231.

Sossin, W. S. and DesGroseillers, L. (2006). Intracellular trafficking of RNA in neurons. *Traffic* **7**, 1581-1589.

Sun, Q.-Q., Zhang, Z., Sun, J., Nair, A. S., Petrus, D. P. and Zhang, C. (2014). Functional and structural specific roles of activity-driven BDNF within circuits formed by single spiny stellate neurons of the barrel cortex. *Front. Cell. Neurosci.* **8**, 372.

Takei, N., Kawamura, M., Hara, K., Yonezawa, K. and Nawa, H. (2001). Brain-derived neurotrophic factor enhances neuronal translation by activating multiple initiation processes: comparison with the effects of insulin. *J. Biol. Chem.* **276**, 42818-42825.

Takei, N., Inamura, N., Kawamura, M., Namba, H., Hara, K., Yonezawa, K. and Nawa, H. (2004). Brain-derived neurotrophic factor induces mammalian target of rapamycin-dependent local activation of translation machinery and protein synthesis in neuronal dendrites. *J. Neurosci.* **24**, 9760-9769.

Tang, S. J., Meulemans, D., Vazquez, L., Colaco, N. and Schuman, E. (2001). A role for a rat homolog of staufen in the transport of RNA to neuronal dendrites. *Neuron* **32**, 463-475.

Tang, S. J., Reis, G., Kang, H., Gingras, A.-C., Sonenberg, N. and Schuman, E. M. (2002). A rapamycin-sensitive signaling pathway contributes to long-term synaptic plasticity in the hippocampus. *Proc. Natl. Acad. Sci. USA* **99**, 467-472.

Tiruchinapalli, D. M., Oleynikov, Y., Kelic, S., Shenoy, S. M., Hartley, A., Stanton, P. K., Singer, R. H. and Bassell, G. J. (2003). Activity-dependent trafficking and dynamic localization of zipcode binding protein 1 and beta-actin mRNA in dendrites and spines of hippocampal neurons. *J. Neurosci.* **23**, 3251-3261.

tom Dieck, S., Kochen, L., Hanus, C., Heumüller, M., Bartnik, I., Nassim-Assir, B., Merk, K., Mosler, T., Garg, S., Bunse, S. et al. (2015). Direct visualization of newly synthesized target proteins in situ. *Nat. Methods* **12**, 411-414.

Tongiorgi, E. (2008). Activity-dependent expression of brain-derived neurotrophic factor in dendrites: facts and open questions. *Neurosci. Res.* **61**, 335-346.

Tongiorgi, E. and Baj, G. (2008). Functions and mechanisms of BDNF mRNA trafficking. *Novartis Found. Symp.* **289**, 136-151; discussion 147-51, 193-5.

Tongiorgi, E., Righi, M. and Cattaneo, A. (1997). Activity-dependent dendritic targeting of BDNF and TrkB mRNAs in hippocampal neurons. *J. Neurosci.* **17**, 9492-9505.

Tongiorgi, E., Righi, M. and Cattaneo, A. (1998). A non-radioactive in situ hybridization method that does not require RNAse-free conditions. *J. Neurosci. Methods* **85**, 129-139.

Tongiorgi, E., Armellin, M., Giulianini, P. G., Bregola, G., Zucchini, S., Paradiso, B., Steward, O., Cattaneo, A. and Simonato, M. (2004). Brain-derived neurotrophic factor mRNA and protein are targeted to discrete dendritic laminas by events that trigger epileptogenesis. *J. Neurosci.* **24**, 6842-6852.

Tongiorgi, E., Sartori, A., Baj, G., Bratina, A., Di Cola, F., Zorzon, M. and Pizzolato, G. (2012). Altered serum content of brain-derived neurotrophic factor isoforms in multiple sclerosis. *J. Neurol. Sci.* **320**, 161-165.

Torre, E. R. and Steward, O. (1992). Demonstration of local protein synthesis within dendrites using a new cell culture system that permits the isolation of living axons and dendrites from their cell bodies. *J. Neurosci.* **12**, 762-772.

Torre, E. R. and Steward, O. (1996). Protein synthesis within dendrites: glycosylation of newly synthesized proteins in dendrites of hippocampal neurons in culture. *J. Neurosci.* **16**, 5967-5978.

Vaghi, V., Polacchini, A., Baj, G., Pinheiro, V. L. M., Vicario, A. and Tongiorgi, E. (2014). Pharmacological profile of brain-derived neurotrophic factor (BDNF) splice variant translation using a novel drug screening assay: a "quantitative code". *J. Biol. Chem.* **289**, 27702-27713.

Verpelli, C., Piccoli, G., Zibetti, C., Zanchi, A., Gardoni, F., Huang, K., Brambilla, D., Di Luca, M., Battaglioli, E. and Sala, C. (2010). Synaptic activity controls dendritic spine morphology by modulating eEF2-dependent BDNF synthesis. *J. Neurosci.* **30**, 5830-5842.

Vicario, A., Colliva, A., Ratti, A., Davidovic, L., Baj, G., Gricman, Ł., Colombrita, C., Pallavicini, A., Jones, K. R., Bardoni, B. et al. (2015). Dendritic targeting of short and long 3′ UTR BDNF mRNA is regulated by BDNF or NT-3 and distinct sets of RNA-binding proteins. *Front. Mol. Neurosci.* **8**, 62.

Wells, D. G., Dong, X., Quinlan, E. M., Huang, Y. S., Bear, M. F., Richter, J. D. and Fallon, J. R. (2001). A role for the cytoplasmic polyadenylation element in NMDA receptor-regulated mRNA translation in neurons. *J. Neurosci.* **21**, 9541-9548.

Xu, X., Miller, E. C. and Pozzo-Miller, L. (2014). Dendritic spine dysgenesis in Rett syndrome. *Front. Neuroanat.* **8**, 97.

Yang, J., Siao, C.-J., Nagappan, G., Marinic, T., Jing, D., McGrath, K., Chen, Z.-Y., Mark, W., Tessarollo, L., Lee, F. S. et al. (2009). Neuronal release of proBDNF. *Nat. Neurosci.* **12**, 113-115.

Zafra, F., Castren, E., Thoenen, H. and Lindholm, D. (1991). Interplay between glutamate and gamma-aminobutyric acid transmitter systems in the physiological regulation of brain-derived neurotrophic factor and nerve growth factor synthesis in hippocampal neurons. *Proc. Natl. Acad. Sci. USA* **88**, 10037-10041.
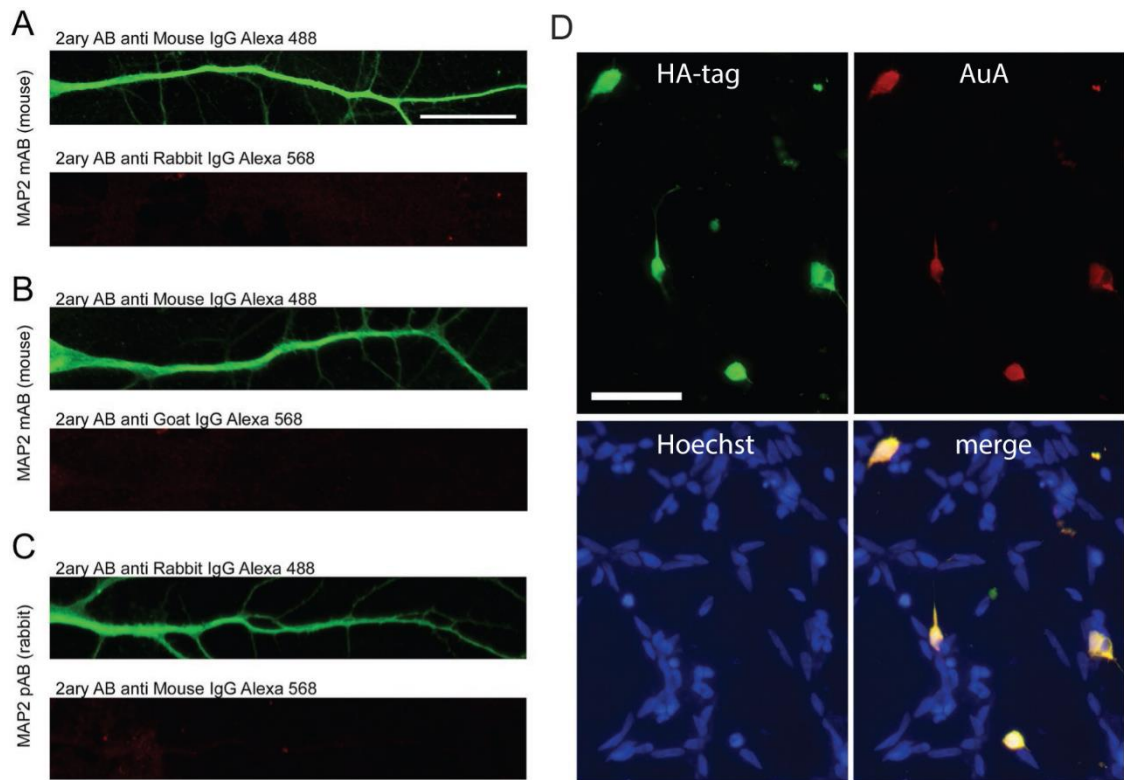
Supplementary Figure 1

A,B,C) Representative images of negative control staining. Hippocampal neurons stained for Map2 and with all secondary antibodies used for immunocytochemistry and immunohistochemistry experiments.D) Immunofluorescence on SK-N-BE cells trasfected with a construct encoding for AuroraA-HA tagged. Green panel: staining with anti-Ha antibody (ABCAM AB18181, 1:500); red panel: anti-AuroraA staining (Cell Signaling n.3092, 1:200); blue panel: Hoechst staining used to highlight nuclei; bottom right panel: merge between the three channels. Scale bar = 50 microns.